

Modelling of Dynamic Crack Propagation in Ice Subjected to Impact Load using Peridynamics

Adem Candaş^{1,2}, Erkan Oterkus², Selda Oterkus², Mehmet Akif Sarıkaya³, C. Erdem İmrak¹

¹ Faculty of Mechanical Engineering, Istanbul Technical University, Istanbul, Türkiye

² PeriDynamics Research Centre, Department of Naval Architecture, Ocean and Marine Engineering, University of Strathclyde, Glasgow, UK

³ Eurasia Institute of Earth Sciences, Istanbul Technical University, Istanbul, Türkiye

ABSTRACT

Both marine and terrestrial ice sheets have been dramatically retreating in response to climate warming during recent years. One of the principal ablation mechanisms in an ice shelf is the calving process which is a consequence of crack propagation of pre-existing fractures. Iceberg calving occurs along ice sheets perimeter depending on various crevasses' parameters such as the location, form, and distribution. In this study, a simple rectangular ice structure subjected to impact load is analysed and dynamic crack propagation in the structure is modelled using bond-based Peridynamics (PD) which is a non-local form of classical continuum theory. To investigate the effect of surface crevasses on glacier fracture mechanism and dynamic crack propagation, the proposed material modelling of ice fracture is discussed. Both the amount and depth of crevasses as effective parameters in the fracture of an ice structure have been seen from numerical results obtained by our PD model. Thus, it can be said that Peridynamic theory is a simple and robust method to model and analyse the relation between surface crevasses and crack propagation in a glacier.

KEY WORDS : Dynamic fracture, Ice fracture, Peridynamics

INTRODUCTION

The damage inflicted by climate change on earth and habitats is so severe that it would take nature centuries to repair. In recent years, climate change has caused a significant reduction in the world's ice volume, as reported by the IPCC (IPCC, 2013). Studying the disappearing glaciers of today and conducting a quantitative analysis of their vanishing mechanism is of utmost importance for enhancing future climate predictions (Köse et al., 2019, 2022; Candaş et al., 2020; Žebre et al., 2021). As highlighted in the IPCC's assessment report, glacier mass loss averaged 335 ± 38 gigatons per year between 2006-2015 (IPCC, 2019). The retreat of both marine and terrestrial glaciers has accelerated significantly in recent years due to the warming of the global climate. Glaciers crack and break in expected manners as they move. Crevasses

have significance in the creation of moulins, the breaking off of icebergs at ice margins, and the tearing apart of ice streams at margins (*antarcticglaciers.org*, 2023). Propagation of crevasses due to melting is a crucial process in the transportation of meltwater to the base of a glacier, which may lead to seasonal accelerations when basal sliding is enhanced (Zwally et al., 2002). The fracture pattern of ice plays a role in the disintegration and rapid collapse of ice shelves. The calving process, which is the fracturing and separation of ice from an ice shelf, is one of the primary mechanisms contributing to ice loss in huge amounts (Benn et al., 2007). The calving process is influenced by various parameters such as the location, form, and distribution of crevasses which are the cracks located on the surface of a glacier. Understanding these parameters and their effects on calving is crucial to accurately predict ice loss and its implications. By incorporating these parameters into models of iceberg formation and calving, we can improve our ability to predict ice loss and associated hazards in offshore areas. In turn, this information can inform measures to mitigate the risks posed by icebergs to ships and offshore infrastructure.

The calving process serves as an input parameter for glacier models. It is a complex process influenced by many factors, including glacier velocity, thickness, bed surface, pre-existed crevasses and other factors (DeConto et al., 2021). Crevasses within the ice sheet play a particularly important role in determining the location and timing of calving events. The distribution and orientation of crevasses are influenced by the stresses and strains experienced by the ice sheet, as well as by the presence of other surface features such as melt ponds and surface lakes. In order to improve our understanding of calving and its role in ice loss, it is necessary to develop enhanced methods for monitoring and measuring the behaviour of ice sheets over time. This includes the use of numerical models to simulate calving processes. Therefore, we can gain a more comprehensive understanding of the complex processes driving ice loss in marine and terrestrial ice sheets and develop more accurate predictions of their future behaviour.

Pralong (2005) proposes a continuum damage mechanics model for ice that describes the damage, rheology, and evolution of damaged ice at low stresses. The model is implemented in a finite element code and applied to the prediction of calving processes and shows good agreement with field measurements. Krug et al. (2014) present a new calving model based on a combination of continuum damage mechanics and linear elastic fracture mechanics, which considers both slow sub-critical surface crevassing and rapid propagation of crevasses during calving. Schlemm and Levermann (2019) derived a stress-based parametrization for cliff calving from grounded glaciers whose freeboards exceed the 100 m stability limit derived in previous studies and proposed a cliff-calving law where the calving rate follows a power-law dependence on the freeboard of the ice. Amaral et al. (2020) evaluated six published iceberg calving models against observations from 50 marine-terminating outlet glaciers in Greenland, revealing that the crevasse depth calving model provides the best balance of high accuracy and low sensitivity to imperfect parameter calibration, making it a leading candidate for use in models of the Greenland Ice Sheet. With the help of the ice flow model Elmer/Ice, van Dongen et al. (2020) determined that the water level of the crevasse plays a crucial role in driving the opening rates of crevasses. They underlined that surface meltwater and tides play a significant role in causing crevasses to open, which ultimately leads to major calving events at grounded tidewater glaciers. The process of iceberg calving takes place at the edges of ice sheets and is influenced by factors such as the location, shape, and arrangement of crevasses. This research investigates the dynamic crack propagation in a basic rectangular ice structure subjected to an impact load, using bond-based Peridynamics (PD).

METHODOLOGY

In recent years, there has been a growing interest in using Peridynamics (PD) to model dynamic fracture problems (Candaş et al., 2021; Candaş et al., 2023). PD theory was developed by Silling (2000) and it can address discontinuity issues that arise in classical continuum mechanics. PD is particularly useful in regions where cracks are forming and propagating in a material, as traditional equations based on partial derivatives are not valid in these areas. PD's equation of motion is valid in both continuity and discontinuity regions owing to its integral equations. Silling (2000) first presented the bond-based PD theory, which postulates that force density vectors between two material points are parallel and of equal magnitude. In 2007, the theory was extended to state-based PD, which uses unequal force density vectors (Silling et al., 2007). The equation of motion for any material point \mathbf{x} in PD theory is defined using integral equations, as detailed in (Silling and Askari, 2005).

$$\rho \ddot{\mathbf{u}}(\mathbf{x}, t) = \int_{\mathcal{H}_x} \mathbf{f}(\mathbf{u}(\mathbf{x}', t) - \mathbf{u}(\mathbf{x}, t), \mathbf{x}' - \mathbf{x}) dV_{x'} + \mathbf{b}(\mathbf{x}, t), \quad (1)$$

where \mathbf{x}' is one of the family members of the material point \mathbf{x} which is inside the horizon, \mathcal{H}_x . The δ is the radius of the spherical horizon region. \mathbf{f} is the force vector which is mutual between two material points. As shown in Figure 1, \mathbf{u} and \mathbf{u}' are the displacement vectors of \mathbf{x} and \mathbf{x}' , respectively. \mathbf{b} is the body load, ρ is the density, and $dV_{x'}$ is the infinitesimally small volume of point \mathbf{x}' .

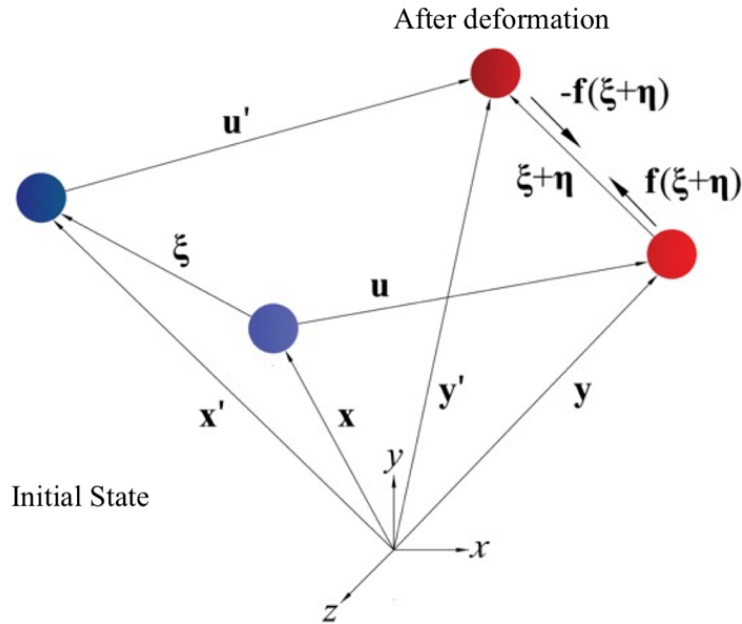


Figure 1. Initial and deformed state of two material points (Candaş et al., 2023)

In Figure 1, $\xi = \mathbf{x}' - \mathbf{x}$ is the relative position vector at the initial state while $\eta + \xi = \mathbf{y}' - \mathbf{y}$ is after deformation. Therefore $\eta = \mathbf{u}(\mathbf{x}', t) - \mathbf{u}(\mathbf{x}, t)$ is the relative displacement vector (Madenci and Oterkus, 2014). The stretch of a bond can be expressed by considering the relative displacement between material points as follows,

$$s = \frac{(\mathbf{y}' - \mathbf{y}) - (\mathbf{x}' - \mathbf{x})}{\mathbf{x}' - \mathbf{x}} = \frac{|\boldsymbol{\xi} + \boldsymbol{\eta}| - |\boldsymbol{\xi}|}{|\boldsymbol{\xi}|}. \quad (2)$$

The bonds connecting two material points are represented as an elastic spring within a micro-elastic material through this equation. Thus, the micro-potential function in the bond can be expressed as a scalar in bond-based Peridynamics.

$$w(\boldsymbol{\eta}, \boldsymbol{\xi}) = \frac{1}{2} c s^2 |\boldsymbol{\xi}|, \quad (3)$$

where $c = 12E/\pi\delta^4$ is the bond constant for 3D structures and E is Young's modulus and δ is the radius of the horizon (Madenci and Oterkus, 2014). The \mathbf{f} is the pairwise force function and derivative of the micro-potential function with regard to the relative displacement vector.

$$\mathbf{f}(\boldsymbol{\eta}, \boldsymbol{\xi}) = \frac{\partial w}{\partial \boldsymbol{\eta}}(\boldsymbol{\eta}, \boldsymbol{\xi}) = \frac{\boldsymbol{\xi} + \boldsymbol{\eta}}{|\boldsymbol{\xi} + \boldsymbol{\eta}|} f(|\boldsymbol{\xi} + \boldsymbol{\eta}|, \boldsymbol{\xi}) \quad \forall \boldsymbol{\eta}, \boldsymbol{\xi}. \quad (4)$$

The scalar-valued function f is defined based on the bond constant and bond stretch. The bond between two material points is valid only if the initial reference distance between these points is smaller than the horizon radius. The force function between material points is expressed as a scalar-valued function:

$$f(|\boldsymbol{\xi} + \boldsymbol{\eta}|, \boldsymbol{\xi}) = \begin{cases} cs\mu(t, \boldsymbol{\xi}) & \text{if } |\boldsymbol{\xi}| < \delta \text{ for all } \boldsymbol{\eta}, \\ 0 & \text{otherwise} \end{cases} \quad (5)$$

where $\mu(t, \boldsymbol{\xi})$ is a history-dependent scalar-valued step function. If the bond-stretch $s(t', \boldsymbol{\xi})$ is smaller than the critical-stretch s_c , it is valued as 1, otherwise, 0 which means vanishing of the bond between two material points. The local damage equation represents the ratio of the number of damaged bonds to the total number of bonds for a given material point, which can be expressed as,

$$\varphi(\mathbf{x}, t) = 1 - \frac{\int_{\mathcal{H}_x} \mu(\mathbf{x}, t, \boldsymbol{\xi}) dV_{\boldsymbol{\xi}}}{\int_{\mathcal{H}_x} dV_{\boldsymbol{\xi}}}. \quad (6)$$

It is difficult to solve the integral-based equation of motion of PD analytically. Thus, a numerical solution is constructed by discretizing the continuum body into volumes. The governing equation for a material point k , which considers all points in its horizon, is provided in a discretized form:

$$\rho_k \ddot{\mathbf{u}}_k^n = \sum_j \mathbf{f}(\mathbf{u}_j^n - \mathbf{u}_k^n, \mathbf{x}_j - \mathbf{x}_k) V_j + \mathbf{b}_k^n, \quad (7)$$

where, \mathbf{u}_k^n is the displacement vector for a material point k at the time step n^{th} . The Δx is the constant grid spacing and the volume of material point j is defined as $V_j = (\Delta x)^3$ in a 3D body.

NUMERICAL MODELS

This section presents numerical examples of an impact problem with pre-existing crevasses on a glacier terminus using the bond-based Peridynamic (PD) theory. The applicability of crack definition and bond-based PD implementation for a fracture problem is demonstrated through a single crack case. The impact of the number and length of crevasses on the crack propagation is then examined.

Cuffey and Paterson (2010) explained that snow is typically used to describe material that has not undergone significant changes since it fell, while firn refers to material in a transitional state between snow and ice. Although the original definition of firn was limited to wetted snow that survived one summer without becoming ice, this has since expanded to include altered snow on polar glaciers where there is no melting. However, the broad definition lacks a clear distinction between snow and firn due to the continuous nature of snow transformation, with no abrupt changes in physical properties that could serve as a basis for demarcation. On the other hand, it was also noted by Cuffey and Paterson, the boundary between firn and ice is more distinct than between snow and firn. When the interconnecting air- or water-filled passageways between the firn grains are sealed off, a process called pore close-off, firn becomes glacier ice. This typically happens at a density of around 830 kg m^{-3} . Air is commonly present in glacier ice in the form of bubbles, and when these bubbles are compressed, they contribute significantly to the increase in density. The typical density value of glacier ice is considered to be 917 kg m^{-3} which is valid only at temperatures close to 0°C and under low confining pressures seen in small mountain glaciers and the uppermost layers of ice sheets (Cuffey and Paterson, 2010).

When the elasticity limit of ice is surpassed, it leads to brittle failure and crevasses formation (Herzfeld et al., 2004). There are three types of crevasses: tensile, opening stresses, fracturing and sliding, and tearing (Benn et al., 2007). The strength of ice under tension is affected by factors such as water content, temperature, density, and structure (*antarcticglaciers.org*, 2023). Crevasses can form at the edges of a glacier where the ice is subjected to lateral stresses from the valley walls, particularly in steep areas. However, in this study, we only focus on crevasses that occur at the head of an ice-shelf. These crevasses form due to changes in longitudinal stresses resulting from longitudinal extension in the upper part of the glacier.

We used a rectangular cross section as shown in Figure 2, with dimensions $L = 0.200 \text{ m}$, $W = 0.100 \text{ m}$, and $t = 0.009 \text{ m}$. The distance of the first initial crack from $x = 0$ is $d_i = 0.1 \text{ m}$, and the distance between the cracks is $d_c = 25 \text{ m}$. The length (or depth) of cracks is $l_c = \{0.25, 0.50, 0.75\}$. During simulations, the structure is assumed to be traction-free and at rest. We also assumed the projectile as a rigid body with dimensions; $D = 0.25 \text{ m}$, $H = 0.25 \text{ m}$, and $m = 1.57 \text{ kg}$, with a constant velocity $v = -32 \text{ m/s}$ along the y -axis. We discretized the body with $201 \times 101 \times 9$ material points along x , y , and z -axes, respectively, with a grid size of $\Delta = 0.001 \text{ m}$ in each direction, resulting in a total of 182,709 material points. The horizon's radius is $\delta = 3.015 \times \Delta$, with a timestep $\Delta t = 8.7 \times 10^{-8} \text{ s}$ and with the critical-stretch $s_c = 0.01$. Young's modulus and Poisson ratio were used as 5 GPa and 0.25 , respectively due to the restrictions of bond-based PD on Poisson ratio.

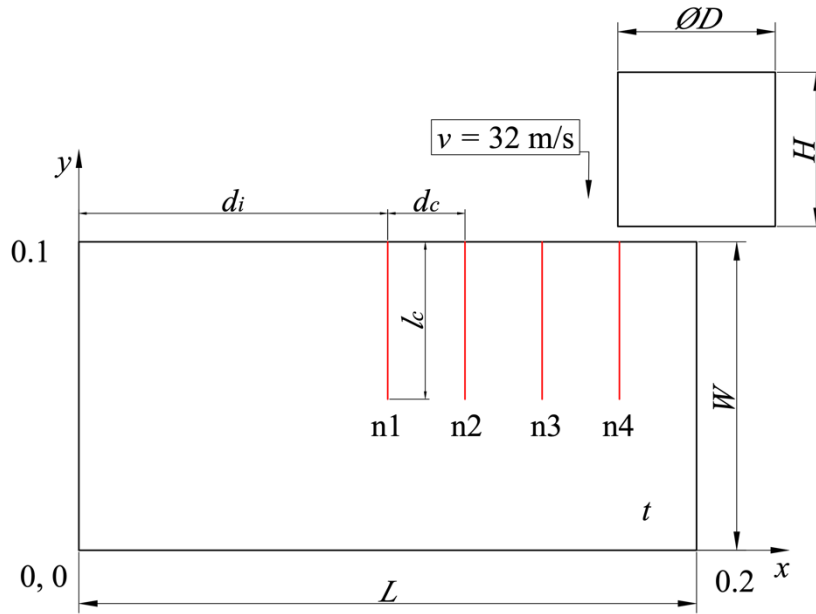


Figure 2. Geometrical definition of model

Schulson (1999) described the variation of Young's modulus of single crystals between 8.6 GPa to 12 GPa depending on the direction near the melting point. The value is 10 GPa for directions within the basal plane. For randomly oriented polycrystals, the typical values of Young's modulus and Poisson's ratio are 9.0 MPa and 0.33 at -5°C . According to Cuffey and Paterson (2010), elastic deformations in a crystalline ice lattice occur due to the stretching and bending of inside bonds. Young's modulus for isotropic polycrystalline ice is approximately 9 GPa. Vazic et al. (2020) modelled sea ice as an isotropic brittle material with Young's modulus of 5 GPa and shear modulus of 2.0625 GPa. The Mode-I fracture toughness of sea ice is given as $0.06 \text{ MPam}^{1/2}$ and ice was considered as a brittle material. Lu et al. (2020) reported an average elastic modulus of 9.584 GPa for ice. Zhang et al. (2021) employed PD to simulate the icebreaking process and used the following ice properties: Young's modulus $E = 52 \text{ MPa}$, Poisson's ratio $\nu = 0.33$, and critical stretch $s_c = 0.0052$.

Figure 3 shows the crack propagation and damage patterns for each model. The models include a varying number of pre-defined cracks that represent crevasses, denoted by "n" and a specific crack length, denoted by "lc". For instance, n2lc50 indicates the presence of two pre-defined crevasses with a length of 0.50 m in the body.

The results presented in Figure 3 depict the screenshots taken at the end of step 1350. It is observed that a crack has initiated in the n1, n2, and n3 models due to the impact of the projectile, even though no previously defined cracks were present in the impacted area. In the n4 models, crack propagations occur from the tip of the predefined crack.

It is noteworthy that the crack initiations in lines n1, n2, and n3 are not due to the pre-existing cracks, but rather the impact itself. Moreover, the angle of crack propagation changes with the increase in crevasse length in the n4 model. This demonstrates that crevasse modelling can be easily achieved using the PD theory. However, it should be acknowledged that the applied impact load does not precisely reflect the natural calving process. In future studies, the glacier's extension on the sea, ice shelf, can be modelled in detail, considering the forces created by seawater and gravity.

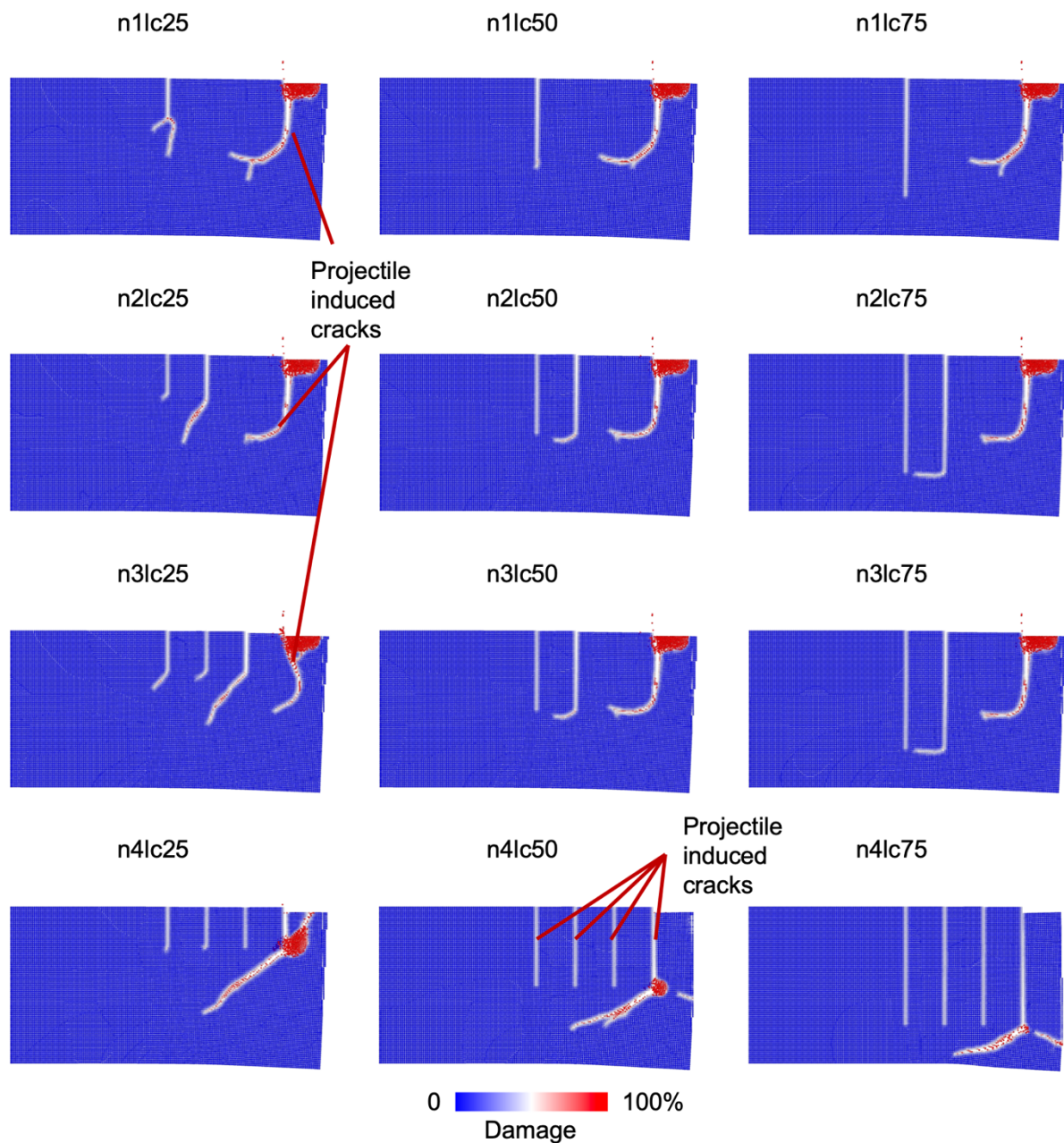


Figure 3. Crack propagation and damage in all models

According to van der Veen (1998), glacier ice is not a linear elastic material and its deformation under stress is described by a non-linear visco-elastic rheology. However, it is possible to use linear elastic fracture mechanics concepts to investigate factors that affect crevasse penetration. Van der Veen (2007) also stated that water-filled crevasses can penetrate cold glaciers within hours to days by adopting concepts based on linear elastic fracture mechanics. The duration of penetration depends on ice thickness and the availability of ponding surface water. Once water-driven crevasse propagation starts, the growth rate is primarily determined by the amount of water flowing into the crevasse, not by ice-mechanical properties such as fracture toughness or the magnitude of the remote tensile stress. Thus, future studies should define a thickness for predefined cracks to accurately represent their structure. Furthermore, the effect of water pressure on crevasses should be taken into account. The state-based PD method can be utilized

to investigate the variation of material properties depending on depth and temperature since glaciers can be viewed as functionally graded materials.

CONCLUSIONS

In the realm of glacial mechanics, the application of linear elastic fracture mechanics to investigate the calving process and the impact of crevasses may yield promising results. Nevertheless, numerous variables must be considered when modelling glacial structures. For instance, glacier density changes with depth, porosity, and temperature, which can be defined parametrically in future studies. However, the values of Young's modulus and Poisson's ratio differ across various studies in the literature and require experimental verification. Material modelling must also account for grain size, anisotropy, and temperature-induced variations in elastic behaviour. Finally, the influence of water pressure within crevasses on fracture propagation should be taken into account, as it is a crucial factor in the models. Further research focusing on these variables is crucial for more accurate predictions of glacial behaviour and calving processes.

ACKNOWLEDGEMENTS

Adem Candaş is supported by the Scientific and Technological Research Council of Turkey (TÜBİTAK) 2219 International Postdoctoral Research Fellowship Program, Project No: 1059B192100891.

REFERENCES

Amaral, T., Bartholomäus, T.C. & Enderlin, E.M., 2020. Evaluation of Iceberg Calving Models Against Observations From Greenland Outlet Glaciers. *Journal of Geophysical Research: Earth Surface*, 125(6). <https://doi.org/10.1029/2019JF005444>.

antarcticglaciers.org, 2023. <https://www.antarcticglaciers.org/glacier-processes/structural-glaciology/> (Accessed: 1 March 2023).

Benn, D.I., Warren, C.R. & Mottram, R.H., 2007. Calving processes and the dynamics of calving glaciers. *Earth-Science Reviews*, 82(3–4), pp. 143–179. <https://doi.org/10.1016/j.earscirev.2007.02.002>.

Candaş, A., Sarıkaya, M.A., Köse, O., Şen, Ö.L. & Çiner, A., 2020. Modelling Last Glacial Maximum ice cap with the Parallel Ice Sheet Model to infer palaeoclimate in south-west Turkey. *Journal of Quaternary Science*, 35(7), pp. 935–950. <https://doi.org/10.1002/jqs.3239>.

Candaş, A., Oterkus, E. & İmrak, C.E., 2021. Dynamic crack propagation and its interaction with micro-cracks in an impact problem. *Journal of Engineering Materials and Technology, Transactions of the ASME*, 143(1), pp. 1–10. <https://doi.org/10.1115/1.4047746>.

Candaş, A., Oterkus, E. & İmrak, C.E., 2023. Modelling and Analysis of Wire Ropes Subjected to Transverse Impact Load using Peridynamic Theory. *Journal of the Faculty of Engineering and Architecture of Gazi University* [Preprint].

Candaş, Adem, Oterkus, E. & İmrak, C.E., 2023. Peridynamic simulation of dynamic fracture in functionally graded materials subjected to impact load. *Engineering with Computers*, 39(1), pp. 253–267. <https://doi.org/10.1007/s00366-021-01540-2>.

- Cuffey, K.M. & Paterson, W.S.B., 2010. *The physics of glaciers, 4th Edition*. Elsevier.
- DeConto, R.M., Pollard, D., Alley, R.B., Velicogna, I., Gasson, E., Gomez, N., Sadai, S., Condrón, A., Gilford, D.M., Ashe, E.L., Kopp, R.E., Li, D. & Dutton, A., 2021. The Paris Climate Agreement and future sea-level rise from Antarctica. *Nature*, 593(7857), pp. 83–89. <https://doi.org/10.1038/s41586-021-03427-0>.
- van Dongen, E., Jouvét, G., Walter, A., Todd, J., Zwinger, T., Asaji, I., Sugiyama, S., Walter, F. & Funk, M., 2020. Tides modulate crevasse opening prior to a major calving event at Bowdoin Glacier, Northwest Greenland. *Journal of Glaciology*, 66(255), pp. 113–123. <https://doi.org/10.1017/jog.2019.89>.
- Herzfeld, U.C., Clarke, G.K.C., Mayer, H. & Greve, R., 2004. Derivation of deformation characteristics in fast-moving glaciers. *Computers and Geosciences*, 30(3), pp. 291–302. <https://doi.org/10.1016/j.cageo.2003.10.012>.
- IPCC, 2013. *Climate Change 2013: The Physical Science Basis. Contribution of Working Group I to the Fifth Assessment Report of the Intergovernmental Panel on Climate Change*. Geneva, Switzerland.
- IPCC, 2019. *IPCC Special Report on the Ocean and Cryosphere in a Changing Climate”. Technical Summary*. Geneva, Switzerland.
- Köse, O., Sarıkaya, M.A., Çİner, A. & Candaş, A., 2019. Late Quaternary glaciations and cosmogenic ³⁶Cl geochronology of Mount Dedegöl, south-west Turkey. *Journal of Quaternary Science*, 34(1), pp. 51–63. <https://doi.org/10.1002/jqs.3080>.
- Köse, O., Sarıkaya, M.A., Çiner, A., Candaş, A., Yıldırım, C. & Wilcken, K.M., 2022. Reconstruction of Last Glacial Maximum glaciers and palaeoclimate in the central Taurus Range, Mt. Karanfil, of the Eastern Mediterranean. *Quaternary Science Reviews*, 291, p. 107656. <https://doi.org/10.1016/j.quascirev.2022.107656>.
- Krug, J., Weiss, J., Gagliardini, O. & Durand, G., 2014. Combining damage and fracture mechanics to model calving. *Cryosphere*, 8(6), pp. 2101–2117. <https://doi.org/10.5194/tc-8-2101-2014>.
- Lu, W., Li, M., Vazic, B., Oterkus, S., Oterkus, E. & Wang, Q., 2020. Peridynamic Modelling of Fracture in Polycrystalline Ice. *Journal of Mechanics*, 36(2), pp. 223–234. <https://doi.org/10.1017/jmech.2019.61>.
- Madenci, E. & Oterkus, E., 2014. *Peridynamic theory and its applications. Peridynamic Theory and Its Applications*. New York, NY: Springer New York. <https://doi.org/10.1007/978-1-4614-8465-3>.
- Pralong, A., 2005. Dynamic damage model of crevasse opening and application to glacier calving. *Journal of Geophysical Research*, 110(B1), p. B01309. <https://doi.org/10.1029/2004JB003104>.
- Schlemm, T. & Levermann, A., 2019. A simple stress-based cliff-calving law. *The Cryosphere*, 13(9), pp. 2475–2488. <https://doi.org/10.5194/tc-13-2475-2019>.

Schulson, E.M., 1999. The structure and mechanical behavior of ice. *JOM*, 51(2), pp. 21–27. <https://doi.org/10.1007/s11837-999-0206-4>.

Silling, S.A., 2000. Reformulation of elasticity theory for discontinuities and long-range forces. *Journal of the Mechanics and Physics of Solids*, 48(1), pp. 175–209. [https://doi.org/10.1016/S0022-5096\(99\)00029-0](https://doi.org/10.1016/S0022-5096(99)00029-0).

Silling, S.A., Epton, M., Weckner, O., Xu, J. & Askari, E., 2007. Peridynamic states and constitutive modeling. *Journal of Elasticity*, 88(2), pp. 151–184. <https://doi.org/10.1007/s10659-007-9125-1>.

Silling, S.A. & Askari, E., 2005. A meshfree method based on the peridynamic model of solid mechanics. *Computers and Structures*, 83(17–18), pp. 1526–1535. <https://doi.org/10.1016/j.compstruc.2004.11.026>.

Vazic, B., Oterkus, E. & Oterkus, S., 2020. In-Plane and Out-of Plane Failure of an Ice Sheet using Peridynamics. *Journal of Mechanics*, 36(2), pp. 265–271. <https://doi.org/10.1017/jmech.2019.65>.

van der Veen, C.J., 1998. Fracture mechanics approach to penetration of surface crevasses on glaciers. *Cold Regions Science and Technology*, 27(1), pp. 31–47. [https://doi.org/10.1016/S0165-232X\(97\)00022-0](https://doi.org/10.1016/S0165-232X(97)00022-0).

van der Veen, C.J., 2007. Fracture propagation as means of rapidly transferring surface meltwater to the base of glaciers. *Geophysical Research Letters*, 34(1). <https://doi.org/10.1029/2006GL028385>.

Žebre, M., Sarıkaya, M.A., Stepišnik, U., Colucci, R.R., Yıldırım, C., Çiner, A., Candaş, A., Vlahović, I., Tomljenović, B., Matoš, B. & Wilcken, K.M., 2021. An early glacial maximum during the last glacial cycle on the northern Velebit Mt. (Croatia). *Geomorphology*, 392, p. 107918. <https://doi.org/10.1016/j.geomorph.2021.107918>.

Zhang, Y., Wang, C., Ye, L. & Tao, L., 2021. Numerical analysis of two different types of icebreaker bows breaking ice by the particle method. *Proceedings of the International Conference on Port and Ocean Engineering under Arctic Conditions, POAC*, 2021-June.

Zwally, H.J., Abdalati, W., Herring, T., Larson, K., Saba, J. & Steffen, K., 2002. Surface melt-induced acceleration of Greenland ice-sheet flow. *Science*, 297(5579), pp. 218–222. <https://doi.org/10.1126/science.1072708>.